

## Measurements of turbulent and periodic flows around a square cross-section cylinder \*

D. F. G. Durão, M. V. Heitor and J. C. F. Pereira

Instituto Superior Tecnico, Mechanical Engineering Dept., P-1096 Lisbon Codex, Portugal

**Abstract.** Laser-Doppler measurements of the velocity characteristics are presented for the turbulent flow around a square cross-section cylinder mounted in a water channel for  $Re = 14000$ . The study involved spectral analysis and digital filtering of the LDV data obtained behind the cylinder. The purpose of the measurements is to separate and quantify the turbulent and the periodic, non-turbulent, motions of the wake flow, in order to improve knowledge of the nature of the fluctuations in the near-wake region of two-dimensional bodies. The results show, for example, that in the zone of highest velocity oscillations the energy associated with the turbulent fluctuations is about 40% of the total energy.

### 1 Introduction

The quasi-periodic nature of the flow around two-dimensional bluff-bodies is relevant for many design purposes, but very little information is available on the details of the aerodynamics of near wake flows.

The present study follows those of Durão et al. (1986 a, b) which provide a basis to understanding the nature of the fluctuations in the wake region of two-dimensional bodies and to assess the accuracy of calculation procedures in recirculating flows. In those previous works detailed laser-Doppler measurements were presented for the turbulent flow around a square cross-section cylinder mounted in a water channel for  $Re = 14,000$ . Also, analogue spectral analysis was conducted by processing the signal obtained by sampling and holding the velocity at each new Doppler burst until another valid signal arrives. The results have shown a single spectral peak at the predominant frequency of 4.7 Hz for  $Re = 14,000$  for the normal velocity fluctuations in the centreline of the obstacle. In agreement with the results of Okajima (1982), the Strouhal number is approximately constant and equal to 0.133 for obstacle heights between 8 and 20 mm in the range  $10^3 < Re < 2 \times 10^4$ . The results have suggested that the fluctuating velocity distributions measured by the laser-Doppler velocimeter are a result

of the time averaging measuring process in which the turbulent and the periodic, non-turbulent, contributions to the total, normal and shear, stresses are not decomposed. Similarly, Yeh et al. (1982) have shown that in the near wake around a strut mounted in a circular pipe, the shape of the radial profiles of the normal stresses is qualitatively similar to that of the turbulent variances, although the magnitude of the peaks of the turbulent variances is about half of the time-averaged measured values. These results suggest that a steady-state numerical calculation of the aerodynamic field requires the modeling of the relative motion of the turbulent and non-turbulent zones, for example, as proposed by Celenligil and Mellor (1985). Also, the calculations of Majundar and Rodi (1985) have shown that the separated turbulent flow past circular cylinders cannot be predicted realistically with a standard steady-flow model ignoring the periodic vortex-shedding motion.

The purpose of the present paper is to separate and quantify the energy associated with the turbulent and the periodic, non-turbulent, motions of the flow previously investigated for  $Re = 14,000$ , in order to bring new physical understanding of the nature of the fluctuations in the near wake region of two-dimensional bodies. Fast Fourier transforms and digital filtering techniques are applied to the output of the laser velocimeter, which was digitised and sampled at a constant frequency.

Section 2 summarizes the flow configuration and the experimental method and gives details of the data processing procedures. Section 3 presents and discusses the new results in the context of the previous works. The last section summarizes the main findings and conclusions.

### 2 Experimental method and accuracy

The experiments were performed on an horizontal,  $120 \times 156$  mm, water tunnel made of perspex with a  $20 \times 20$  mm obstacle,  $H$ , set across the narrow dimension,  $W$ ; and completely spanning the duct as schematically shown by Durão et al. (1986 a, b).

\* A version of the paper was presented at the 10th Symposium on Turbulence, University of Missouri-Rolla, September 22–24, 1986

The results were obtained with the obstacle centered between the top and the bottom of the duct, for a reference velocity of  $U_0 = 0.68$  m/s and a freestream turbulence intensity of 6%. The effects of the proximity of the wall, of the size of the obstacle and of the Reynolds number on the wake-flow have been discussed by Durão et al. (1986 a). Measurements obtained in the tunnel without the obstacle have shown that the flow was symmetric and that the wall boundary layer around the region where the obstacle was located, was 15 mm thick.

The origin of the axial,  $X$ , and vertical,  $Y$ , coordinates in the duct is taken at the centre of the upstream face of the obstacle.

Flow visualization has been conducted by injecting at the upstream face of the obstacle (at  $X = 0$ ,  $Y = 0$ ) fluorescein-sodium, a fluorescent dye found to be an ideal tracer fluid for the present application. Fluorescein-sodium is soluble in water, is used in small concentrations such that density differences are negligible and the contamination of the water with the colour of the fluorescein-sodium dye is slow, so that a good contrast could be maintained without frequent replacement of the water in the system. The flow was illuminated by a sheet of laser light obtained by using a cylindrical lens to spread the laser beam. The light source was a 1 W argon-ion laser in the 488 nm line, under which the fluorescein-sodium fluoresces a bright yellowish-green. Visualization using air bubbles as tracer particles has also been performed using a similar illumination system.

Velocity was measured by a laser-Doppler velocimeter operated in the dual-beam, forward-scatter mode with sensitivity to the flow direction provided by light-frequency shifting from acoustic-optic modulation (Bragg cells). The resulting frequency shift was normally set at 700 kHz. The principal characteristics of the laser-Doppler velocimeter, in particular those of the transmitting optics, are summarized in Table 1.

The light scattered by naturally-occurring centres in the water was collected by a lens (focal length of 200 mm) and focused onto the pinhole aperture (0.3 mm) of a photomultiplier (OEL, type LD-0-810) with a magnification of 1.55. The output of the photomultiplier was band-pass filtered and the resulting signal processed by a laboratory-built frequency counter, as described by Heitor et al. (1984).

**Table 1.** Principal characteristics of the laser Doppler velocimeter

15 mW (nominal) He-Ne laser, wavelength	632.8 nm
focal length of focussing lens	300 mm
beam diameter, at $e^{-2}$ intensity, of laser	1.1 mm
measured half-angle of beam intersection (in air)	4.81°
calculated half-angle of beam intersection (in water)	3.61°
fringe separation (line pair spacing)	3.77 $\mu$ m
calculated dimensions of measuring volume, at $e^{-2}$ intensity (major and minor axis of ellipsoid in water)	3.489; 0.220 mm
velocimeter transfer constant	0.2650 MHz/(ms <sup>-1</sup> )

Estimates of the maximum inaccuracy and precision associated with each measurement have been presented by Durão et al. (1986 b). Systematic errors due to non-turbulent Doppler ambiguity and velocity bias effects are small and the largest statistical (random) errors were of 0.5 and 3%, respectively for the mean and variance values, according to the analysis referred by Yanta and Smith (1978) for a 95% confidence interval.

The concentration of the naturally-occurring scattering centers in water, which give rise to Doppler signals, is such that the probability of finding more than one particle in the measuring volume of the anemometer is negligibly small: hence the occurrence of Doppler signals is a discrete, rather than a continuous process. This fact eliminates power spectrum aliasing but limits the spectral analysis of the velocity characteristics, once fast Fourier transform methods cannot be directly used. Several methods have been proposed for spectral estimation of LDV information (see, for example, Srikantaiah and Coleman 1985, Lading 1985, Saxena 1985) and the procedure adopted here has consisted in frequency analysing the output of the counter after to be digitalized, transferred to the memory of a MicroVAX II computer, and sampled at a constant frequency of 2 kHz, using linear interpolation between the measurements. This procedure requires a mean sampling rate at least three times the Nyquist rate and, as also discussed by Saxena (1985), limits the frequency range for spectral analysis but is considerably better than the sample-and-hold technique. Adrian and Yao (1985) have shown that holding results in missing high frequency information, with a low pass filter frequency equal to half of the mean data rate and that the attenuation is about 10% at a frequency equal to one-twentieth of the data rate. In the present study the data rate varied between 200 and 2000 Hz and, therefore, is high enough to avoid biasing errors and render the analysis valid at the low frequency range of interest here (i.e., about 5 Hz).

Two procedures have been used to quantify the relative contributions of the turbulent and the periodic, non-turbulent, motions to the total flow field. First, the velocity fields were decomposed into a sum of mean, periodic, and random velocity components by matching the mean values of the amplitude of the periodic and measured signals, as described by Yeh et al. (1982). For a component  $U_i(t)$ :

$$U_i(t) = \bar{U}_i + \sqrt{2} u_{p_i} \sin(2\pi f t + \phi) + u'_i(t) \quad (1)$$

where  $\bar{U}_i$  is the mean velocity,  $u_{p_i}$  the rms amplitude of the velocity component occurring at the fundamental frequency of the vortex shedding,  $f$ , with a corresponding phase of  $\phi$ , and  $u'_i(t)$  is the remaining turbulence velocity. Higher harmonics of the periodic flow have not been detected. Second, digital band-reject filters were used. Chebyshev filters of 7th order (e.g., Bendat and Piersol 1971) were chosen with an attenuation of 10 dB at the fundamental frequency,  $f$ , and of 3 dB at  $f \pm 1$  Hz. The accuracy of the variance of the filtered signals is limited mainly by the mean data rate and the finite

sample size and is estimated to be within 9% of the maximum values measured.

### 3 Experimental results and discussion

Part of this study was devoted to observing the periodic flow structure around the square cross-section cylinder which might, at least qualitatively, explain the vortex shedding mechanism. The visualization experiments of Fig. 1 a show a large amplitude vortex-street wake as a result of the mutual interaction between the top and bottom separating shear layers. It is postulated by Gerrard (1966) and discussed by Bearman (1984) that the vortex continues to grow, fed by circulation from its connected shear layer, until it is strong enough to draw the opposing shear layer across the near wake. In Fig. 1 the interaction between one shear layer and the vortex forming on the opposite side of the wake is clearly seen. The streaklines of Fig. 1 b identify the accelerating flow upstream of, and around, the obstacle, the recirculating flow behind the obstacle and the development of the wake flow far downstream.

The important features of the time-averaged flow are summarised by the distribution of mean flow streamlines and the turbulent kinetic energy, discussed in detail by

Durão et al. (1986 b) and shown in Figure 2 a and b. The stream function was defined considering the flow two-dimensional, which is a particularly good approximation at the central plane of the channel where the measurements were made. In general, the mean flow characteristics are similar to those of other separated flows with a free stagnation point reported in the literature. Here, the stagnation occurs at  $X/H = 1.83$ .

The distribution of the turbulent kinetic energy,  $k$ , was calculated on the basis of local isotropy, i.e.  $k = 3/4(\overline{u'^2} + \overline{v'^2})$ . The contours reveal distributions which are qualitatively similar to those in the confined arrangements of Fujii et al. (1978), McKillop and Durst (1986), Taylor and Whitelaw (1984) and Yeh et al. (1982) and in the unconfined flows of Durão and Whitelaw (1978) and Durão et al. (1984). The shear layer surrounding the recirculation bubble is a region of intense velocity fluctuations: the level of turbulent kinetic energy rises as the downstream distance increase, with maximum values around the reverse flow boundary at the stagnation zone; the individual stresses are anisotropic in that  $\overline{v'^2}$  is largest close to the rear stagnation point, while the highest values of  $\overline{u'^2}$  lie along the curved shear layer.

Comparison with the flows listed above indicates that the magnitude of the peaks are significantly higher than those reported in non-periodic turbulent wakes; on the contrary,

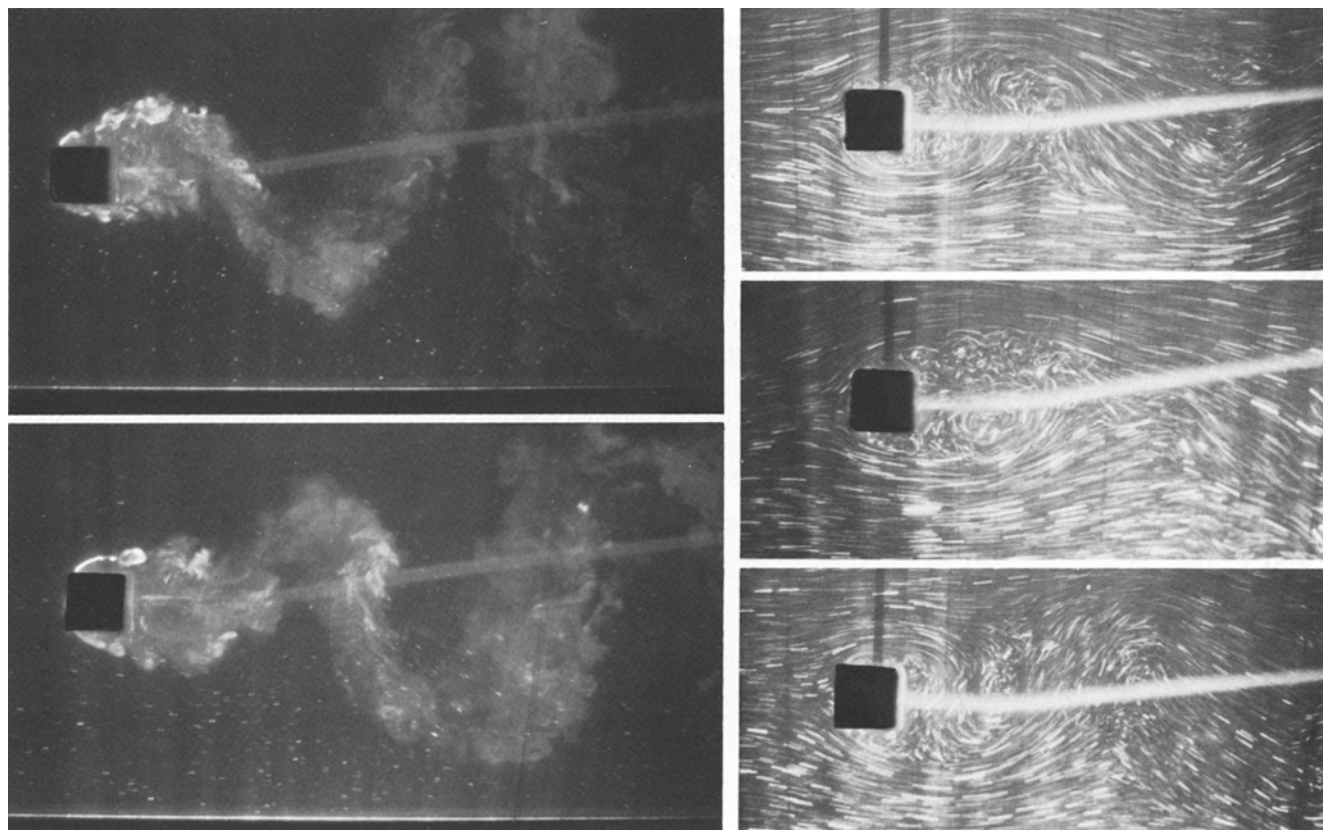


**Fig. 1 a and b.** Visualization of the flow around the obstacle for  $Re = 14,000$ ; **a** flow visualization by injecting a solution of fluorescein-sodium at the upstream face of the obstacle (at  $X = 0, Y = 0$ ); **b** flow visualization using air bubbles as tracer particles

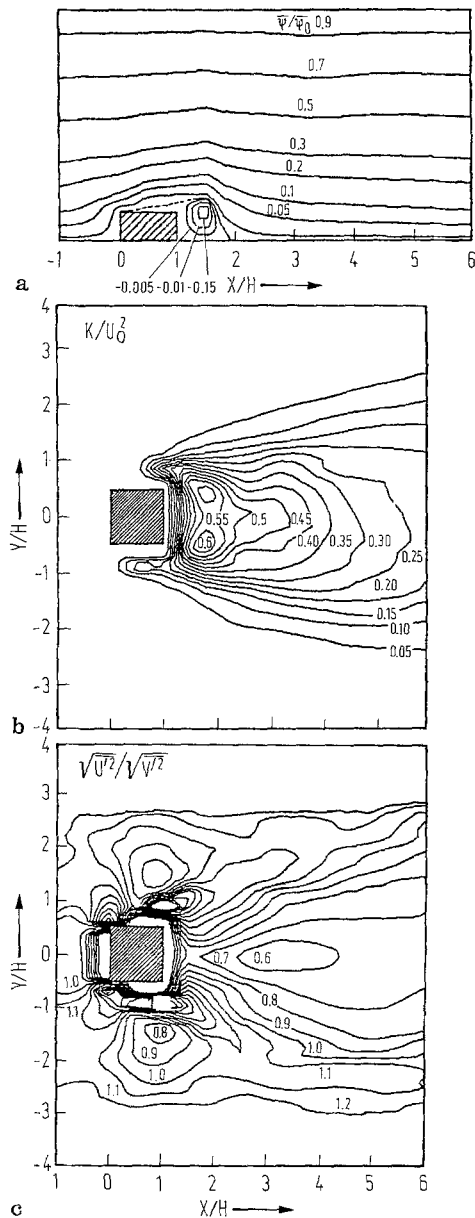


**Fig. 2a–c.** The time-averaged mean and turbulent flow field for  $Re = 14,000$ ; **a** mean flow streamlines.  $\Psi_0 = \int_0^L \bar{U}(y) dy$ ;  $L$  – half length of the channel, 78 mm (see Durão et al. 1986 b); **b** distribution of turbulent kinetic energy,  $K/U_0^2$  (Durão et al. 1986 b); **c** distribution of turbulence anisotropy,  $\sqrt{u'^2}/\sqrt{v'^2}$

the values are similar to those reported by Yeh et al. (1982) and Bradbury (1976), and explained as the result of vortex shedding. Also, the structure parameters calculated by Durão et al. (1986 b), such as  $\overline{u'v'}/U_{max}^2$ ,  $R_{uv}$  and  $\overline{u'v'}/K$ , show that the shear stress in the present near-wake flow is higher than that in non-periodic turbulent shear layers and suggest the existence of local periodic oscillations.

The distribution of the levels of measured anisotropy is shown in Figure 2c. The Reynolds stresses are particularly anisotropic along the separating shear layer where  $\sqrt{u'^2}/\sqrt{v'^2} = 2.2$  at  $Y/H = (0.875 \pm 0.025)$ . On the centreline the

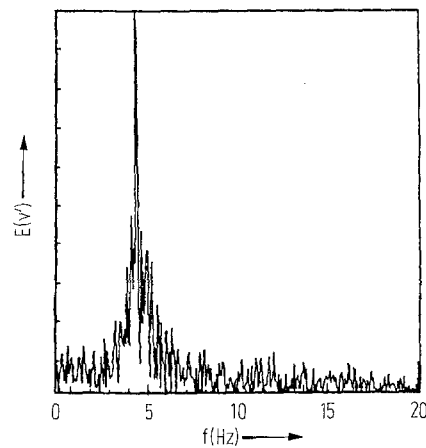


**Fig. 3.** Digital power spectra of normal velocity fluctuations in the centreline of the wake flow for  $Re = 14,000$ ;  $X/H = 5$ ;  $Y/H = 0$ ;  $\bar{V}/U_0 = 0$ ;  $f = 4.7 H_z$

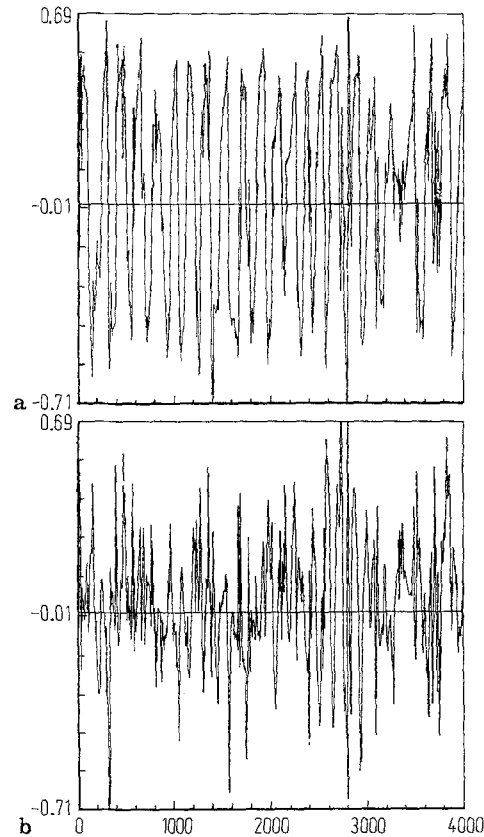


**Fig. 4 a and b.** Time-resolved normal velocity fluctuations at  $X/H = 5$ ,  $Y/H = 0$  (flow conditions of Fig. 3); **a** measured signal, **b** filtered signal (using a band-reject filter centered at the predominant frequency)

level of turbulence anisotropy reaches a value of  $\sqrt{u'^2}/\sqrt{v'^2} = 0.45$  at  $X/H = 3.25$  ( $\sqrt{u'^2}/\sqrt{v'^2} = 0.65$  at stagnation).

Figure 3 shows a characteristic digital spectral analysis of LDV data (at  $X/H = 5$ ,  $Y/H = 0$ ) and confirms the oscillating nature of the present flow with a fundamental frequency of 4.7 Hz for  $Re = 14,000$ . Higher harmonics could not be detected particularly far downstream of the obstacle, as also

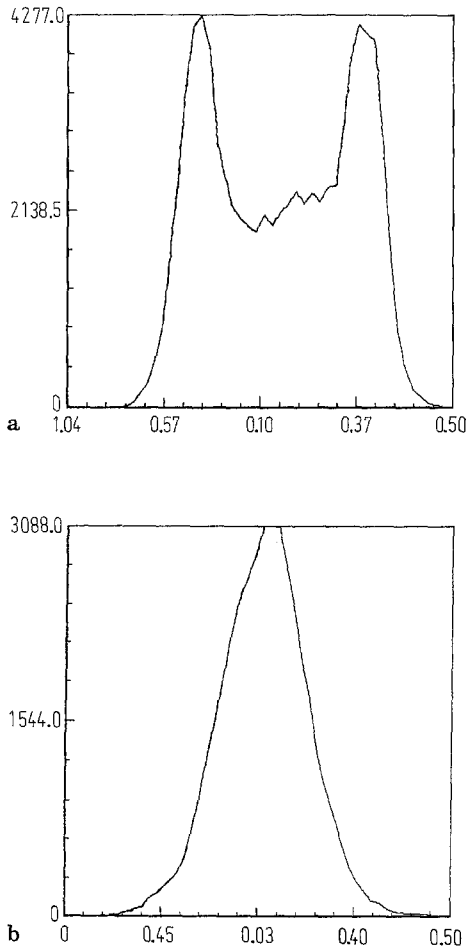


**Fig. 5 a and b.** Histogram of normal velocity fluctuations at  $X/H = 5$ ,  $Y/H = 0$  (flow conditions of Fig. 3); **a** measured signal, **b** filtered signal (using a band-reject filter centered at the predominant frequency)

pointed out by Maclenan and Vincent (1982) and Castro (1985). Yeh et al. (1982) have observed in the spectrum of the normal velocity fluctuations in the vicinity of a strut mounted in a pipe that energy at the first harmonic is also important, although it becomes negligible far downstream of the obstacle.

The time-resolved output of the counter over 4 s is shown in Fig. 4 a after to be linearly interpolated and resampled with a constant frequency of 2 kHz. The signal follows a “noisy” sinusoidal wave with a corresponding bimodal probability density function, shown in Fig. 5 a.

Band-reject filtering of the measured signal centered at the predominant frequency have allowed to decompose the turbulent fluctuations from the periodic oscillations. The former are shown in Fig. 4 b and are characterized by a near-Gaussian probability density function (Fig. 5 b), with the mean value of the measured signal but with a variance 37% of that measured.

This analysis has been extended to the whole flow field and Fig. 6 a and b shows the centreline development of  $\overline{u'^2}$  and  $\overline{v'^2}$ , measured and filtered using the two procedures defined previously, together with the distribution of the mean axial velocity. The variance of the band reject filtered signal of the normal velocity fluctuations,  $\overline{v'^2}$ , is consistently lower than that of the turbulent fluctuations decomposed from a sine wave because of the large attenuation of the former in the band  $f \pm 1$  Hz. Nevertheless, the agreement between the two filtered curves reveals the well defined sinusoidal signals measured for the normal velocity.

The time-resolved axial velocity fluctuations,  $U(t)$ , exhibit comparatively low intensity peaks in the power spectrum and badly defined sinusoidal signals, such that only the band reject filter could be used to decompose the turbulent and the periodic axial flows.

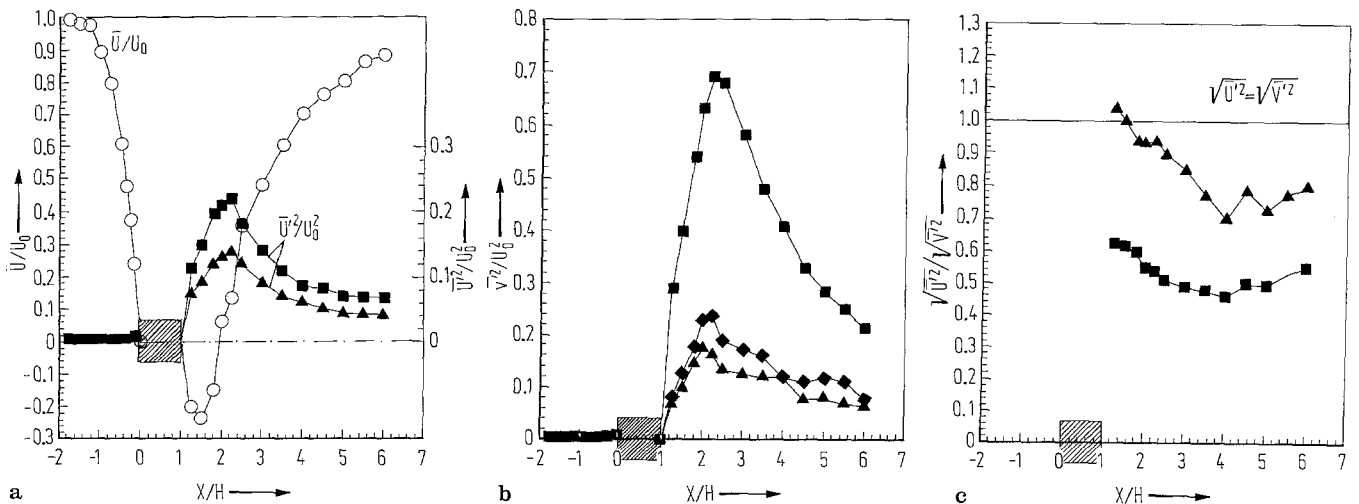


**Fig. 6 a–c.** Centreline distribution of velocity characteristics,  $Re = 14,000$ ; **a** axial velocity:  $\circ \overline{U}/U_0$ ,  $\blacksquare \overline{u'^2}/U_0^2$  measured,  $\blacktriangle \overline{u'^2}/U_0^2$  filtered (band-reject); **b** normal velocity:  $\blacksquare \overline{v'^2}/U_0^2$  measured,  $\blacktriangle \overline{v'^2}/U_0^2$  filtered (band-reject),  $\blacklozenge \overline{v'^2}/U_0^2$  decomposed from sine wave, as in Eq. (1); **c** turbulence anisotropy:  $\blacksquare \sqrt{\overline{u'^2}}/\sqrt{\overline{v'^2}}$  measured,  $\blacktriangle \sqrt{\overline{u'^2}}/\sqrt{\overline{v'^2}}$  filtered (band-reject)

In general, the results show that the filtered distributions of  $\overline{u'^2}$  and  $\overline{v'^2}$  reveal the same trends of the measured signal with the maximum values located in the same points, but with lower values, respectively about 30% and 65% for the normal and axial velocity fluctuations. As a consequence, the anisotropy of the filtered Reynolds stresses has decreased substantially, as shown in Fig. 6c: turbulence anisotropy (i.e.  $\sqrt{\overline{u'^2}}/\sqrt{\overline{v'^2}}$ ) on the centerline has a maximum value of 0.7 in comparison with 0.45 of the measured signal.

Figure 7 shows vertical profiles of filtered and measured normal and shear stresses downstream of the stagnation point, at  $X/H = 2.5$ , and agrees with the above analysis: the qualitative trends are maintained but the filtered variances are lower. In particular, the peaks in the filtered profiles of  $\overline{u'^2}$  are still located around the separation streamline and are associated with the maximum transversal gradients of  $\bar{U}$  but are about 53% of the measured values. It is interesting to note that in the context of the analysis reported by Durão et al. (1986 b), the maximum filtered values of  $\overline{u'^2}$  and  $\overline{v'^2}$  are similar to those reported in non-periodic turbulent wakes, for example by Fujii et al. (1978), Mckillop and Durst (1986) and Taylor and Whitelaw (1984).

The decrease in the values of the filtered turbulent energy relative to those measured is associated to a comparatively large variation between the measured and filtered shear stress. The peaks in the filtered profiles of  $\overline{u'v'}$  are about 40% of the measured ones, and have the order of magnitude of the values measured by, for example, Durst and Mckillop (1986).

At the location of maximum shear stress, the correlation coefficient  $R_{uv}$  decreased from 0.54 to 0.47 and the ratio between filtered shear stress and turbulent kinetic energy is 0.31 and, therefore, similar to the value of 0.30 reported by Bradshaw et al. (1967) and Harsha and Lee (1970) for non-periodic turbulent shear flows. Around  $Y/H = 1.50$ , where

the maximum measured correlation coefficients have reached values close to unity, the maximum filtered coefficients are about 0.50. At these locations the filtered values of  $\overline{u'v'}/K$  are close to 0.30 while the measured values are as high as 0.70. In summary, these structure parameters show that the values of the filtered shear stress in the present near-wake flow are characteristic of “well-behaved” turbulent shear flows, while the measured values result from the existence of local periodic oscillations. In the zones of maximum velocity oscillations the energy associated with the turbulent fluctuations is about 40% of the total energy. These results imply that the steady-state numerical calculation of the separated flow behind two-dimensional bodies requires modeling of the periodic vortex-shedding motion.

#### 4 Conclusions

Spectral analysis and digital filtering of LDV data have provided detailed information of the structure of the turbulent flow around a square cross-section cylinder for  $Re = 14,000$ . The following is a summary of the more important findings and conclusions of this work.

The shear layer surrounding the recirculation bubble behind the cylinder, for  $Re = 14,000$ , is a region of intense velocity fluctuations with unusually high values of the Reynolds (normal and shear) stresses, explained as the result of vortex shedding, with a frequency of 4.7 Hz. The analysis of the flow requires consideration of both turbulent and periodic oscillations.

In the zones characterized by the highest velocity oscillations the energy associated with the turbulent fluctuations is about 40% of the total energy. The turbulent profiles of  $\overline{u'^2}$ ,  $\overline{v'^2}$  and  $\overline{u'v'}$  exhibit the same trends of the measured

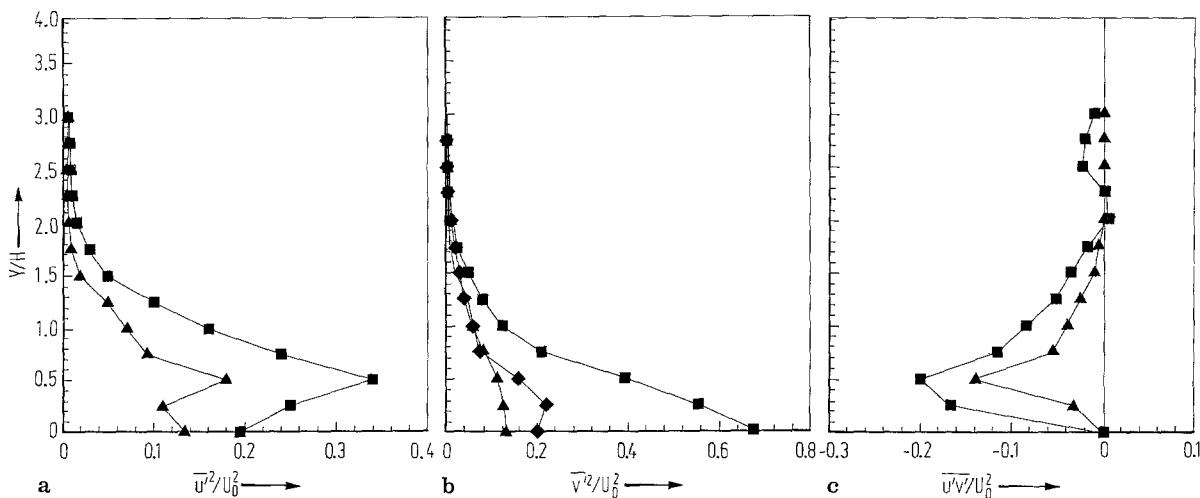


**Fig. 7 a–c.** Vertical profiles of normal and shear Reynolds stresses at  $X/H = 2.5$  (upper half profiles),  $Re = 14,000$ ; **a** axial velocity:  $\blacksquare \overline{u'^2}/U_0^2$  measured,  $\blacktriangle \overline{u'^2}/U_0^2$  filtered (band-reject); **b** normal velocity:  $\blacksquare \overline{v'^2}/U_0^2$  measured,  $\blacktriangle \overline{v'^2}/U_0^2$  filtered (band-reject),  $\blacklozenge \overline{v'^2}/U_0^2$  decomposed from sine wave, as in Eq. (1); **c** shear stress:  $\blacksquare \overline{u'v'}/U_0$  measured,  $\blacktriangle \overline{u'v'}/U_0$  filtered (band-reject)

quantities with the maximum values located in the same points, but with values respectively about 65%, 30% and 40% of the time-averaged measurements. The levels of turbulence anisotropy are smaller than the measured ones, with maximum values in the centreline about 0.70.

In general, the experiments reported here quantify the relative importance of the turbulent and non-turbulent motions of the flow around two-dimensional bluff-bodies. The results show that the structure of the turbulent motion is qualitatively similar to that of more classical shear flows.

### Acknowledgements

We are pleased to record our thanks to Mr. J. Martins and colleagues in the Centro de Electronica Aplicada in the Dept. of Electrical Engineering for help in the frequency analysis and digital filtering techniques used throughout this work. The assistance of Mr. J. Brisson with the laboratory computers is gratefully acknowledged. Thanks are also due to Mrs. Susana Valério for her speedy typing of this report. The experiments were partially supported by Stiftung Volkswagenwerk and by NATO research grant number 602, and made at the Centro de Termodinamica Aplicada e Mecanica dos Fluidos de Universidade Tecnica de Lisboa.

### References

- Adrian, R. J.; Yao, C. S. 1985: Power spectra of fluid velocities measured by laser Doppler velocimetry. ASME, Winter Annual Meeting, Miami Beach/FL, November 15–22, 1985
- Bearman, P. W. 1984: Vortex shedding from oscillating bluff bodies. *Ann. Rev. Fluid Mech.* 16, 195–222
- Bendat, J. S.; Piersol, A. G. 1971: *Random data: analysis and measurement procedures*. New York: Wiley-Interscience
- Bradbury, L. J. S. 1976: Measurements with a pulsed-wire and a hot-wire anemometer in the highly turbulent wake of a normal flat plate. *J. Fluid Mech.* 77, 473–497
- Bradshaw, P.; Ferriss, D. H.; Atwell, N. P. 1967: Calculation of boundary layer development using the turbulent energy equation. *J. Fluid Mech.* 28, 593–616
- Castro, I. P. 1985: Time-domain measurements in separated flows. *J. Fluid Mech.* 150, 183–201
- Celenligil, M. C.; Mellor, G. L. 1985: Numerical solution of two-dimensional turbulent separated flows using a Reynolds stress closure model. *J. Fluids Eng.* 107, 467–476
- Durão, D. F. G.; Durst, F.; Firmino, F. 1984: Velocity characteristics of the flow around cones. Proc. 2nd Int. Symp. on Appl. of LA to Fluid Mech. Pap. 15.2, Lisbon, July 1984
- Durão, D. F. G.; Heitor, M. V.; Pereira, J. C. F. 1986 a: The flow around a squared obstacle. 67th AGARD-PEP Conference, Philadelphia, May 19–23
- Durão, D. F. G.; Heitor, M. V.; Pereira, J. C. F. 1986 b: A Laser anemometry study of separated flow around a squared obstacle. In: *Laser anemometry in fluid mechanics III* (eds Adrian, R. J. et al.), pp. 227–243. LADOAN-IST, Lisbon, Portugal
- Durão, D. F. G.; Whitelaw, J. H. 1978: Velocity characteristics of the flow in the near wake of a disc. *J. Fluid Mech.* 85, 369–385
- Edwards, R. V.; Jensen, A. S. 1983: Particle-sampling statistics in laser anemometers: sample-and-hold and saturable systems. *J. Fluid Mech.* 133, 397–411
- Fujii, S.; Gomi, M.; Eguchi, K. 1978: Cold flow tests of a bluff-body flame stabilizer. *J. Fluids Eng.* 100, 323–332
- Gerrard, J. H. 1966: The mechanism of the formation region of vortices behind bluff bodies. *J. Fluid Mech.* 25, 401–413
- Harsha, P. T.; Lee, S.C. 1970: Correlation between turbulent shear stress and turbulent kinetic energy. *AIAA J.* 8, 1508–1510
- Heitor, M. V.; Laker, J. R.; Taylor, A. M. K. P.; Vafidis, C. 1984: Instruction manual for the FS “model 2” Doppler-frequency counter. Imperial College, London, Dept. Mech. Eng., Rep. FS/84/10
- Lading, L. 1985: Spectral analysis versus counting. ASME, Winter Annual Meeting, Miami Beach/FL, November 17–22
- Majumdar, S.; Rodi, W. 1985: Numerical calculations of turbulent flow past circular cylinders. 3rd Symp. on Numerical and Physical Aspects of Aerodynamic Flows. Long Beach/CA, January 21–24
- Maclennan, A. S. M.; Vincent, J. H. 1982: Transport in the near aerodynamic wakes of flat plates. *J. Fluid Mech.* 120, 185–197
- McKillop, A. A.; Durst, F. 1986: A laser anemometry study of separated flow behind a circular cylinder. In: *Laser anemometry in fluid mechanics II* (eds Adrian, R. J. et al.) LADOAN-IST, Lisbon, Portugal
- Okajima, A. 1982: Strouhal numbers of rectangular cylinders. *J. Fluid Mech.* 123, 379–398
- Saxena, V. 1985: Power spectrum estimation from randomly sampled velocity data. ASME Winter Annual Meeting, Miami Beach/FL, November 17–22
- Srikantaiah, D. V.; Coleman, H. W. 1985: Turbulence spectra from individual realization laser velocimetry data. *Exp. Fluids* 3, 35–44
- Taylor, A. M. K. P.; Whitelaw, J. H. 1984: Velocity characteristics in the turbulent near wakes of confined axisymmetric bluff bodies. *J. Fluid Mech.* 139, 391–416
- Yanta, W. J.; Smith, R. A. 1978: Measurements of turbulent-transport properties with a laser Doppler velocimeter. AIAA Pap. 73–169, 11th Aerospace Science Meeting, Washington/DC
- Yeh, T. T.; Robertson, B.; Mattar, W. M. 1982: LDV measurements near a vortex shedding strut mounted in a pipe. ASME Winter Annual Meeting, Phoenix/AZ, November, 14–19

Received July 27, 1987